Modeling the Dynamic Equilibrium between Oligomers of $(AlOCH_3)_n$ in Methylaluminoxane (MAO). A Theoretical Study Based on a Combined Quantum Mechanical and Statistical Mechanical Approach

E. Zurek, T. K. Woo, T. K. Firman, and T. Ziegler*

Department of Chemistry, University of Calgary, Calgary, Alberta, Canada T2N 1N4

Received July 31, 2000

Density functional theory (DFT) has been used to calculate the energies of 36 different methylaluminoxane (MAO) cage structures with the general formula $(MeAlO)_n$, where n ranges from 4 to 16. A least-squares fit has been used to devise a formula which predicts the total energies of the MAO with different *n*'s giving an rms deviation of 4.70 kcal/mol. These energies in conjunction with frequency calculations based on molecular mechanics have been used to estimate the finite temperature enthalpies, entropies, and free energies for these MAO structures. Furthermore, formulas have been devised which predict finite temperature enthalpies and entropies for MAO structures of any *n* for a temperature range of 198.15−598.15 K. Using these formulas, the free energies at different temperatures have been predicted for MAO structures where *n* ranges from 17 to 30. The free energy values were then used to predict the percentage of each *n* found at a given temperature. Our calculations give an average *n* value of 18.41, 17.23, 16.89, and 15.72 at 198.15, 298.15, 398.15, and 598.15 K, respectively. Topological arguments have also been used to show that the MAO cage structure contains a limited amount of square faces as compared to octagonal and hexagonal ones. It is also suggested that the limited number of square faces with their strained Al−O bonds explain the high molar Al:catalyst ratio required for activation. Moreover, in this study we outline a general methodology which may be used to calculate the percent abundance of an equilibrium mixture of oligomers with the general formula $(X)_n$.

1. Introduction

In 1980, Sinn and Kaminsky discovered that the addition of water to systems such as $Cp_2ZrMe_2/AlMe_3$ caused this rather inactive reaction system to become highly active in ethene polymerization.[1] It was suspected that partial hydrolysis of $AlMe_3$ (TMA) brought about the formation of methylaluminoxane (MAO). It was further postulated that the role of the MAO/TMA mixture in this system was to act as cocatalyst. Equation 1 illustrates the commonly accepted role of MAO as the catalyst activator. Equation 2 indicates the possible role of the product cation as a catalyst in olefin polymerization.

$$(\eta_5\text{-}C_5H_5)_2MMe_2 + MAO \rightarrow [(\eta_5\text{-}C_5H_5)_2MMe]^+ + [(MAO)Me]^- \quad M = Ti, Zr \quad (1)$$

$$[(\eta_5\text{-}C_5H_5)_2MMe]^+ + n[CH_2{=}CH_2] \rightarrow [(\eta_5\text{-}C_5H_5)_2M[CH_2CH_2]_nCH_3]^+ \quad (2)$$

The high activity imparted by MAO has caused it for many years to be one of the most industrially important activators in single-site or metallocene-catalyzed olefin polymerization. Yet, despite this fact the structure (structures) of MAO remain largely unknown. The characterization of MAO by NMR spectroscopy has been hindered by disproportionation reactions at high temperatures and association in solution yielding a mixture of different oligomers with multiple equilibria. Moreover, the characterization cannot be carried out using X-ray diffraction due to the fact that it is not possible to isolate crystalline samples.[2]

The determination of the structure of MAO can be linked to the determination of the structures of alumoxanes in general. Alumoxanes are intermediates in the hydrolysis of organoaluminum compounds to aluminum hydroxides. They were originally proposed as consisting of a linear **1** or cyclic **2a**−**c** chain structure (Figure 1) which were composed of alternating three-coordinate aluminum and two-coordinate oxygen atoms.[3] The first crystallographic evidence for the presence of four-coordinate aluminum atoms was given by Atwood and co-workers in their structural determination of the $[Al_7O_6Me_{16}]^-$ anion **3**.[4] This result encouraged many groups to propose structures consisting of fused four- or six-membered rings or both (**4**) for that of MAO.[3] While these structures were more reasonable than those of **1** and those similar to **2a**−**c**, they still contained a peripheral aluminum atom which remained three-coordinate. Methyl bridges and/or the presence of trimethylaluminum groups were suggested,[3] but these resulted in structures whose chemical formula substantially deviated from the generally accepted formula of "pure" MAO, $(MeAlO)_n$, where *n* is an integer.

Replacement of the methyl substituents in MAO with bulkier *tert*-butyl groups made the first structural determination of alkylalumoxanes possible. Barron and co-workers synthesized a series of compounds $[(^tBu)Al(\mu_3\text{-}O)]_n$, where $n = 6-9$ and 12.[2,5] These correspond to structures **5**−**8**, respectively (Figure 2). The synthesis of these compounds led to the suggestion that

(1) Sinn, H.; Kaminsky, W.; Vollmer, H. J.; Woldt, R. *Angew. Chem.* **1980**, *92*, 396.
(2) Mason, M. R.; Smith, J. M.; Bott, S. G.; Barron, A. R. *J. Am. Chem. Soc.* **1993**, *115*, 4971.
(3) Pasynkiewicz, S. *Polyhedron* **1990**, *9*, 429.
(4) Atwood, J. L.; Hrncir, D. C.; Priester, R. D.; Rogers, R. D. *Organometallics* **1983**, *2*, 985.
(5) Harlan, C. F.; Mason, M. R.; Barron, A. R. *Organometallics* **1994**, *13*, 2957.

10.1021/ic000845b CCC: $20.00
Published on Web 12/19/2000

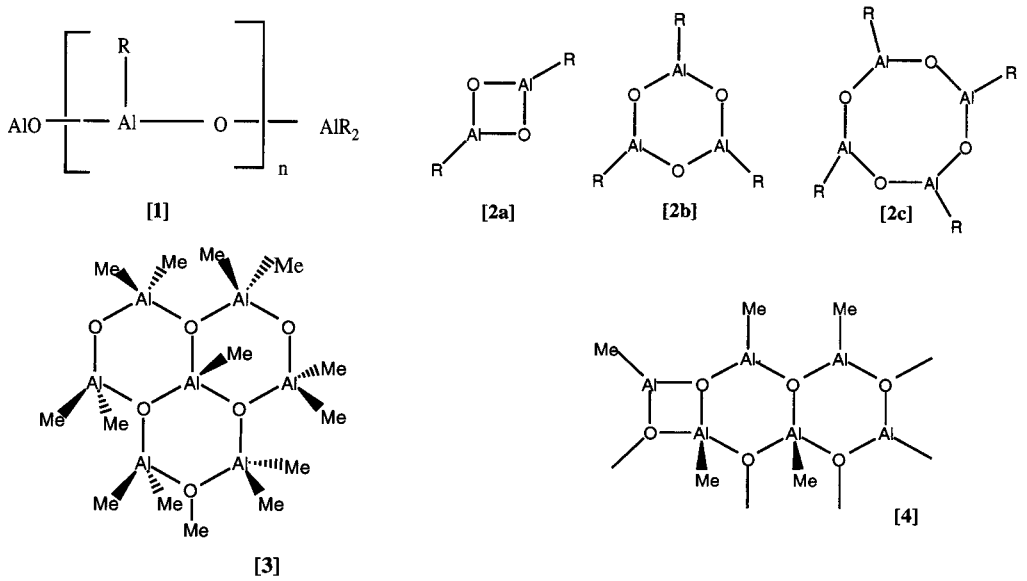

Figure 1. Proposed structures for aluminoxanes.

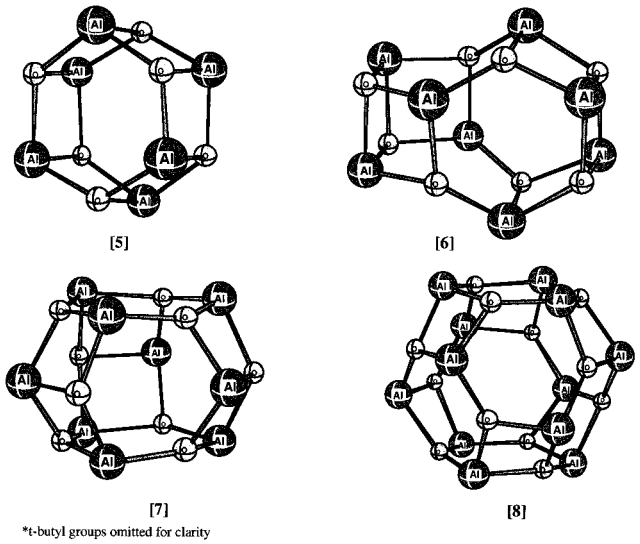

Figure 2. Barron's synthesized $[(^t\text{Bu})\text{Al}(\mu_3\text{-O})]_n$ compounds.

MAO has a three-dimensional cage structure. Within these cage structures four-coordinate aluminum centers bridged by three-coordinate oxygen atoms were thought to predominate.[2] Barron and co-workers have also proposed a topological relationship for the prediction of the structures of $[(^t\text{Bu})\text{Al}(\mu_3\text{-O})]_n$ and $[(^t\text{Bu})\text{Ga}(\mu_3\text{-S})]_n$ cages.[5] For the structures which they synthesized they noted that the number of square faces is always equal to 6, while the number of hexagonal faces is equal to $n - 4$.[5] They have also proposed two possible growth relationships for such compounds.[5]

Barron's $[(^t\text{Bu})\text{Ga}(\mu_3\text{-S})]_n$ cubane underwent structural rearrangements ($n = 6-8$), yet under extreme conditions.[2] However, in the case of MAO, it has been proposed that the cages undergo such rearrangements under normal conditions, as seen in the following equation, where x, y, and z are integers:

$$(\text{MeAlO})_x \leftrightarrow (\text{MeAlO})_y \leftrightarrow (\text{MeAlO})_z \qquad (3)$$

It was known that species of exceptional Lewis acidity are found in MAO solutions, but four coordinate aluminum centers are not thought of as being exceptionally Lewis acidic. Barron and co-workers found that indeed they are and developed the concept of latent Lewis acidity (LLA). LLA is a consequence of the ring strain present in the cluster. If it is assumed that four-coordinate aluminum and three-coordinate oxygen atoms prefer tetrahedral and trigonal planar geometries, respectively, then a qualitative determination of the LLA of a caged compound may be found by calculating the sum of the angular distortions from the ideal.[6] Work has also been done on quantitatively establishing the most acidic of Barron's *tert*-butyl compounds.[7]

As has been mentioned previously, the characterization of the structure of MAO via NMR spectroscopy has not been successful. Yet, NMR and other spectroscopic methods have been used to give further clues as to the structure(s) and role of MAO. In most cases these methods have been used to give an estimate of the size range for a typical MAO oligomer. For example, the line widths of ^{27}Al NMR have predicted that, for $[\text{AlOMe}]_n$, n ranges between 9 and 14 at high temperatures and between 20 and 30 at ambient conditions.[8] EPR studies have been performed via the addition of a spin probe to a MAO solution. Once again, line widths coupled with line intensities were used to find the radius of a MAO structure. This method found that n ranges between 14 and 20.[9]

It is well-known that there exists residual TMA (trimethylaluminum) in all MAO solutions. It is accepted that TMA participates in an equilibrium with different MAO oligomers.[1] However, here we will focus upon establishing a model for a pure (TMA free) MAO solution, although such a system has not been established experimentally. A subsequent paper will focus on MAO-containing TMA. To study real MAO (MAO + TMA solution) it is first necessary to study pure MAO. Currently we are performing this work, using some of the data and methodology presented here.

The objective of this paper is to establish the percent abundance of different MAO structures. Ultimately, it is the Gibbs free energy which determines the stability of a given

(6) Harlan, C. J.; Bott, S. G.; Barron, A. R. *J. Am. Chem. Soc.* **1995**, *117*, 6465.
(7) Koide. Y.; Bott, S. G.; Barron, A. R. *Organometallics* **1996**, *15*, 5514.
(8) Babushkin, D. E.; Semikolenova, N. V.; Panchenko, V. N.; Sobolev, A. P.; Zakharov, V. A.; Talsi, E. P. *Macromol. Chem. Phys.* **1997**, *198*, 3845.
(9) Talsi, E. P.; Semikolenova, N. V.; Panchenko, V. N.; Sobolev, A. P.; Babushkin, D. E.; Shubin, A. A.; Zakharov, V. Z. *J. Mol. Catal. A: Chem.* **1999**, *139*, 131.

structure. The Gibbs free energy is given as

$$G_T(n) = H_T(n) - TS_T(n) \quad (4)$$

where $H_T(n)$ is the enthalpy at temperature T for $(AlOMe)_n$ and $S_T(n)$ the corresponding entropy.

Section 3.1 discusses different structural alternatives (sheets, cages, fused cages) showing that caged structures are energetically the most stable. Section 3.2 derives formulas which are important in determining the topologies of caged structures. Section 3.3 discusses energetic considerations and proposes a method by which they can be predicted. In section 3.4 we discuss and provide methods to estimate enthalpic corrections, and in section 3.5 the same is done for entropies. Finally, section 3.6 examines the Gibbs free energy and percent abundance of different MAO structures.

2. Computational Details

The density functional theory calculations were carried out using the Amsterdam density functional (ADF) program version 2.3.3 developed by Baerends et al.[10] and vectorized by Ravenek.[11] The numerical integration scheme applied was developed by te Velde et al.,[12] and the geometry optimization procedure was based on the method of Verslius and Ziegler.[13] For total energies and geometry optimizations the gradient-corrected exchange functional of Becke[14] and the correlation functional of Perdew[15] were utilized in conjunction with the LDA parametrization of Vosko et al.[16] The electronic configurations of the molecular systems were described by a double-ζ STO basis set with polarization functions. A 1s frozen core was used for carbon and oxygen, while an [Ar] frozen core was used for aluminum. A set of auxiliary s, p, d, f, and g STO functions centered on all nuclei was used to fit the molecular density and represent Coulomb and exchange potentials in each SCF cycle.[17] Single-point numerical differentiation of energy gradients were used for frequency calculations.

UFF2[18,19] was used to calculate entropic and finite temperature enthalpy corrections to the Gibbs free energy. It was necessary to reparametrize the force field for our specific system. The original and reparametrized values are presented in Tables 1.1−1.3 of the Supporting Information.

3. Results and Discussion

3.1. Energetics of Sheet/Caged/Fused-Caged Structures. Despite the fact that experiment has provided evidence that MAO consists of three-dimensional cage structures, it was decided that a preliminary investigation on the relative stability of sheet, caged, and fused-caged structures ought to be performed. These results would then allow us to determine which subset of structures ought to be studied in depth. Figure 3 affords a selection of the sheet and fused-caged structures.

First of all, it must be noted that during the geometry optimization of the fused-caged structure the bonds corresponding to five coordinate Al and four coordinate O atoms broke

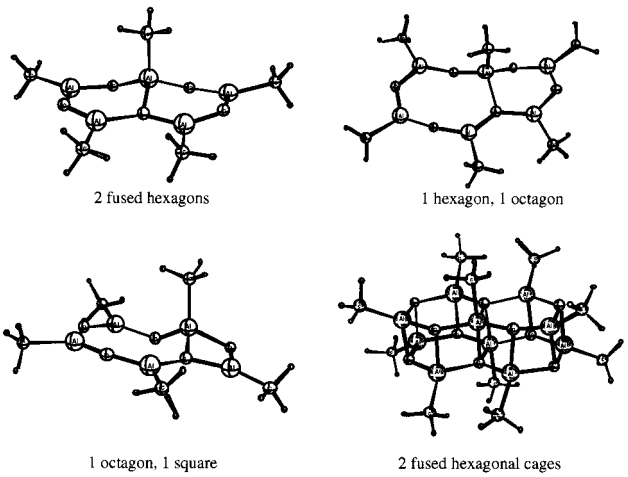

Figure 3. A selection of sheet and fused-caged structures.

Table 1. Binding Energies/Monomer for Sheet Structures

structure	BE/monomer (kcal/mol)	structure	BE/monomer (kcal/mol)
square	−61.62	2 hexagons	−80.18
hexagon	−77.33	1 square, 1 hexagon	−77.29
octagon	−78.83	1 hexagon, 1 octagon	−79.27
decagon	−78.59	1 square, 1 octagon	−78.49
dodecagon	−78.30	2 octagons	−79.35

giving simply a caged structure. This shows that such structures are unstable alternatives for MAO.

The electronic binding energy per monomer unit is defined as

$$\mathrm{BE}(n) = (1/n)(E[(\mathrm{AlOMe})_n] - nE[\mathrm{AlOMe}]) \quad (5)$$

It gives the energy which is gained per monomer (AlOMe unit) when a certain geometry is formed from n monomers. The lower the binding energy per monomer, the more stable the given structure is. Table 1 gives the binding energies per monomer unit for sheet structures. The last five entries correspond to two fused rings.

The first thing which must be noted is that when single-ring structures are considered, the binding energy per monomer decreases until it reaches a minimum for an octagonal ring, before increasing again. The decrease in binding energy must first be attributed to the fact that as the ring becomes larger the O−Al−O and Al−O−Al angles approach values which correspond more closely to those associated with an Al in a trigonal planar environment and an O in a bent environment. As the ring size increases, these angles deviate more from the ideal and the binding energy increases. For the fused-ring structures it is important to note that the binding energy per monomer appears to reach a plateau at approximately −80 kcal/mol.

Next, a preliminary investigation of the binding energies of caged structures was performed. This data can be found in Table 2. With the exception of $(AlOMe)_4$, the other structures correspond to **5**−**8** shown in Figure 2 (the MAO analogues of Barron's synthesized structures). What is important to note is that even for a very strained structure such as $(AlOMe)_4$, the binding energy per monomer is approximately 9 kcal/mol lower than for any of the sheet structures. Hence, this preliminary investigation indicates that caged MAO structures consisting of three coordinate oxygen and four coordinate aluminum atoms are much more energetically stable than sheet or fused-caged structures.

(10) (a) Baerends, E. J.; Ellis, D. E.; Ros, P. *Chem. Phys.* **1973**, *2*, 41. (b) Baerends, E. J.; Ros, P. *Chem. Phys.* **1973**, *2*, 52.
(11) Ravenek, W. *Algorithms and Applications on Vector and Parallel Computers*; te Riele, H. J. J., Dekker, T. J., vand de Horst, H. A., Eds.; Elservier: Amsterdam, 1987.
(12) (a) te Velde, G.; Baerends, E. J. *Comput. Chem.* **1992**, *99*, 84. (b) Boerringter, P. m.; te Velde, G.; Baerends, E. J. *Int. J. Quantum Chem.* **1998**, *33*, 87.
(13) Verslius, L.; Ziegler, T. *J. Chem. Phys.* **1988**, *88*, 322.
(14) Becke, A. D. *Phys. Rev. A.* **1988**, *38*, 3098.
(15) Perdew, J. P. *Phys. Rev. B.* **1986**, *33*, 8822.
(16) Vosko, S. H.; Wilk, L.; Nusair, M. *Can. J. Phys.* **1980**, *58*, 1200.
(17) Krijn, J.; Baerends, E. J. *Fit Functions in the HFS-Method*; Free University of Amsterdam: Amsterdam, 1984.
(18) Casewit, A. K.; Colwell, K. S.; Rappe, A. K. *J. Am. Chem. Soc.* **1992**, *114*, 10046.
(19) Casewit, C. J.; Colsell, K. S.; Rappe, A. K. *J. Am. Chem. Soc.* **1992**, *114*, 10035.

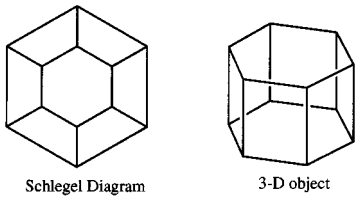

Figure 4. Schlegel diagram and corresponding three-dimensional object.

Table 2. Binding Energy/Monomer for Caged Compounds

structure	BE/monomer (kcal/mol)	structure	BE/monomer (kcal/mol)
$(AlOMe)_4$	−88.73	$(AlOMe)_9$	−100.17
$(AlOMe)_6$	−95.93	$(AlOMe)_{12}$	−102.30
$(AlOMe)_8$	−99.05		

Accordingly, in our investigation of possible MAO geometries it was decided to focus on three-dimensional caged structures. When such a structure is considered, it must be noted that the cage compound itself consists of polygonal faces. Due to the fact that these MAO cages must consist of alternating Al and O atoms, it is clear that such a polygonal face must consist of an even number of atoms. It is not possible within such a study to look at all possible types of faces. Thus, it was decided that caged compounds comprised of square, hexagonal, and octagonal faces would be considered. Later we shall present arguments based on general principles that point to square and hexagonal faces as being the most likely building blocks for caged MAO structures.

3.2. Mathematical Relationships. To construct MAO cage structures, it is first necessary to gain some insight into the construction of polyhedrons consisting of square, hexagonal, and octagonal faces. Within this section, we first of all propose a mathematical method which may be used to construct such polyhedrons. All of the MAO structures on which explicit calculations have been performed have been created using this method. Next, we shall derive a formula which relates the number of square faces to the number of octagonal faces found within a polyhedron. This result will prove useful in explaining the large ratio of Al:catalyst needed in order for polymerization to occur. Finally, we will derive mathematical relationships which will be used later on in order to construct large MAO cages.

A convenient way by which one can construct polyhedrons is via the drawing of Schlegel diagrams.[20] A Schlegel diagram is a projection of a three-dimensional object onto a plane surface. An example of such a diagram is shown in Figure 4. On the left-hand side a Schlegel diagram is shown, with the three-dimensional object which it corresponds to shown on the right. Within this study, the different possible MAO cage structures were constructed via the use of Schlegel diagrams.

Despite the fact that it is not possible to derive all of the possible connectivities present in a polyhedron corresponding to a given number of atoms, some assertions can be made. The first deals with the relationship between the number of square, hexagonal, and octagonal faces comprising a given polyhedron.

From the mathematical study of polytopes, it is known that[20]

$$F + P = C + 2 \tag{6}$$

where F is the number of faces of a given polyhedron, P is the number of points within the polyhedron, and C is the number of connectivities. In this case, P corresponds to the number of atoms within the caged structure, N. Within the cage structure itself each atom bonds to three others. Yet, to find the number of connectivities, this must be divided by two since each connectivity belongs to two atoms. Hence, C is equal to $1.5N$. Thus, eq 6 simplifies to

$$F = 0.5N + 2 \tag{7}$$

Also, it must be noted that each atom belongs to three faces. Thus, if O, H, and S correspond to the number of octagonal, hexagonal, and square faces within a given cage structure, we have the following relation:

$$(8/3)O + (6/3)H + (4/3)S = N \tag{8}$$

Furthermore, the following trivial relationship is true:

$$O + H + S = F \tag{9}$$

If one equates eqs 7 and 9 and then substitutes eq 8 for N, it is found that

$$S = O + 6 \tag{10}$$

Equation 10 gives us a relationship between the number of octagonal and square faces within a MAO cage. It also shows that the minimum amount of square faces which can exist in such a polyhedron is 6 and that this occurs when the number of octagonal faces is 0, that is when the polyhedron is made up solely of square and hexagonal faces.

Other relationships which have been derived apply to the case when only square and hexagonal faces are present. Within such a polyhedron there are only four environments within which each atom (point) may be found. They are the following: a = the number of atoms which are part of 3 square faces; b = the number of atoms part of 2 square and 1 hexagonal face; c = the number of atoms part of 1 square and 2 hexagonal faces; d = the number of atoms part of 3 hexagonal faces.

Despite the fact that $a-d$ are unknown for a given N, what is known is the number of square faces and hexagonal faces along with the number of atoms comprising each face (4 and 6, respectively). Thus, the quantity $4S + 6H$ is known for a given N. Since each atom is part of three faces, we have that

$$4S + 6H = 3N \tag{11}$$

Furthermore, it is clear that

$$a + b + c + d = N \tag{12}$$

And thus that

$$3a + 3b + 3c + 3d = 3N \tag{13}$$

Using eqs 11 and 13 we have that

$$3a + 2b + b + c + 2c + 3d = 4S + 6H \tag{14}$$

But the only terms which contribute to the square faces are $3a$, $2b$, and c. This is because b corresponds to the number of atoms bonded to 2 square and 1 hexagonal face and c to the number of atoms bonded to 1 square and 2 hexagonal faces etcetera. The same reasoning may be used to determine that the only terms which contribute to the hexagonal faces are b, $2c$, and $3d$. Moreover, since the structures which we are

(20) Coxeter, H. S. M. *Regular Polytopes*, 2nd ed.; Macmillian Co.: New York, 1963.

considering consist of only six square faces, the following equations may be determined:

$$3a + 2b + c = 24 \tag{15}$$

$$b + 2c + 3d = 6H \tag{16}$$

Take into consideration a MAO cage which simply consists of square and hexagonal faces. As has been shown, the number of square faces present in this instance is always equal to 6. Then, as the cage grows the number of hexagonal faces increases while the number of square faces stays the same. Thus, for a large cage it can be imagined that the probability that an atom is bonded to 3 square faces becomes very small. Similarly, so does the probability that an atom is bonded to 2 square faces and 1 hexagonal face. Hence, in eqs 15 and 16 a and b can be put to zero. Thus, it becomes trivial to solve for the types of connectivities present in a MAO cage. Later on, this method shall be used to generate large MAO structures. This does not guarantee that such a structure can indeed exist. For confirmation, a Schlegel diagram must be drawn.

3.2.1. Alternative Derivation of Eq 15. Descartes showed that[20] in a polyhedron if the face angles at a vertex amount to $360° - \delta$, where δ is known as the deficit, then

$$\Sigma\delta = 720° \tag{17}$$

Within our structures the deficits for $a-d$ are 90, 60, 30, and 0°, respectively. Hence, by **17**

$$90°a + 60°b + 30°c = 720° \tag{18}$$

Simplifying,

$$3a + 2b + c = 24 \tag{19}$$

which is just eq 15.

3.3. Energetic Considerations. The potential energies of 36 different $(AlOMe)_n$ structures, where n ranges between 4 and 16, were determined via DFT level calculations. The optimized structures and energies are shown in Figure 1 and Table 2 of the Supporting Information. The Cartesian coordinates are given in Figure 2 of the Supporting Information. Some representative structures composed of square and hexagonal faces are shown in Figure 5. For $(AlOMe)_{14}$ only the most stable structural alternative is shown. Figure 6 displays the isomers which were found for $(AlOMe)_8$. The geometries of all structures were found via drawing a Schlegel diagram and next constructing the corresponding three-dimensional structure.

It was determined that the stability of a given MAO is heavily dependent upon the structure of the cage and, specifically, upon the bonding environment present. Hence, a least-squares fit was done to predict the energies of the MAO structures, using the bonding environments as an index. The details of this fit can be found in the appendix. This fit resulted in the following energy expression for any given MAO structure:

$$\begin{aligned} E(n) = &-373.57(3S) - 377.49(2S + H) - \\ &381.13(2H + S) - 381.80(3H) - 377.14(2S + O) - \\ &380.59(2O + S) - 381.03(H + O + S) - \\ &378.86(2H + O) - 365.51(2O + H) \end{aligned} \tag{20}$$

where $3S$ denotes the number of atoms belonging to three square faces, $2S + H$ the number of atoms belonging to two square and one hexagonal face, and so on. $E(n)$ is in kcal/mol. None of the structures which we have considered contained an atom in a $3O$ environment, due to the fact that in order for such an environment to be present, the cage would have to be quite large. Hence, the coefficient for $3O$ is missing in the fit above. The root-mean-square deviation of this fit for the total energy is 4.70 kcal/mol. The fit was checked on $(AlOMe)_{14}$ from Figure 5. The predicted and calculated energies differed by 5.51 kcal/mol. Figure 7 shows the predicted and calculated energy values for the 10 $(AlOMe)_{12}$ isomers. The x-axis corresponds to the structure number, and the y-axis, to the energy. The overall trend is reproduced, with only slight deviations.

Moreover, it must be noted that the coefficients pertaining to each specific bonding environment provide a means by which one can gauge the stability of a particular environment. The more negative the coefficient, the more stable the environment. Hence, the order of stability is, in decreasing order, $3H > 2H + S > H + O + S > 2O + S > 2H + O > 2S + H >$

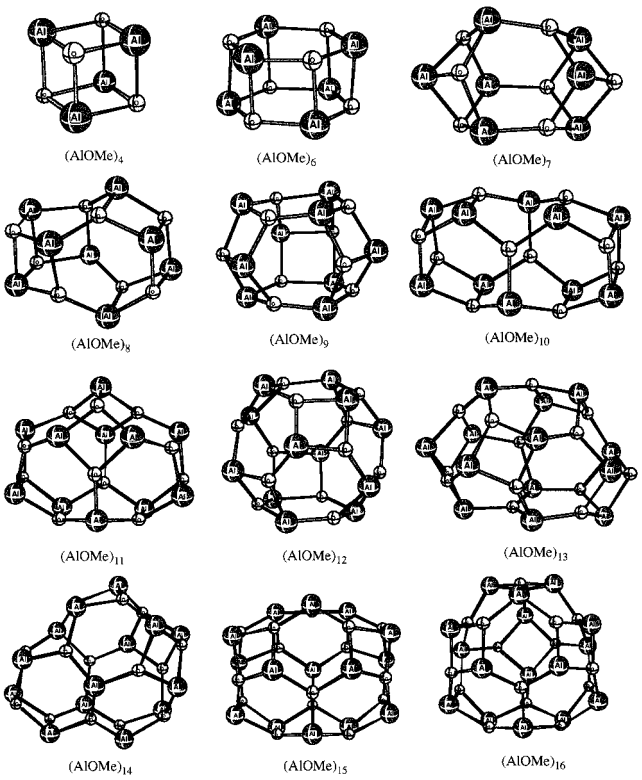

Figure 5. MAO cage structures composed of square and hexagonal faces only for $(AlOMe)_4$–$(AlOMe)_{16}$.

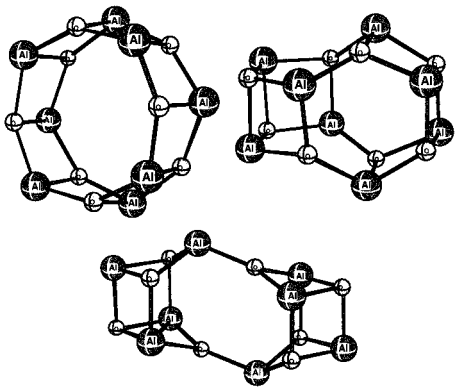

Figure 6. Different isomers for $(AlOMe)_8$.

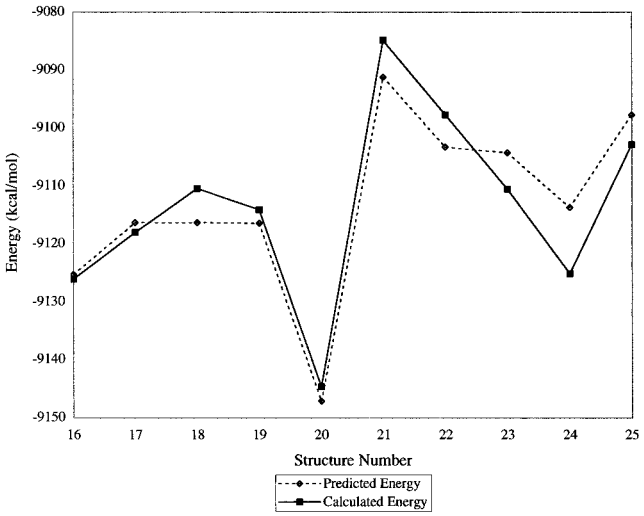

Figure 7. Predicted and calculated energies for $(AlOMe)_{12}$ isomers.

$2S + O > 3S > 2O + H$. Thus, an atom bonded to three hexagonal faces is the most stable, while an atom bonded to two octagonal and one hexagonal face is the least stable.

It is also interesting to note that the structures which are composed simply of square and hexagonal faces have the lowest energies for a given n with the exception of $(AlOMe)_{10}$ where another structure is 0.38 kcal/mol more stable. This can be attributed to the fact that the number of square faces within a structure is equal to the number of octagonal faces plus 6. Thus, the minimum possible number of square faces occurs when no octagonal faces are present. The square faces exhibit a large amount of ring strain therefore destabilizing the structure. Hence, the structures with the least amount of square faces present for a given n, are most stable, energetically.

Figure 8 shows the energy per monomer unit as a function of n for the structures composed simply of square and hexagonal faces. For n =17, 18, 20, 21, 25, and 30, the bonding environments were found using eqs 15 and 16, verified via the drawing of the corresponding Schlegel diagram, and eq 20 was used to predict the energies. Since these energies were predicted, error bars are present.

The first notable aspect of Figure 8 is that the energy per monomer approaches a plateau as n increases. Equations 15 and 16 show that in general as a MAO cage increases in size the number of atoms found in a $2H + S$ environment is 24, while the number of atoms in a $3H$ environment increases as a function of n. Equation 20 then assigns certain coefficients to atoms in each environment. Thus, for large n, the energy of a structure becomes a linear function of n and hence the energy per monomer unit reaches a plateau with increasing n. The graph displays an almost smooth curve, with the exception of three local maxima points which are present at n =7, 10, and 13. More energetically stable structural alternatives for these oligomers could not be found. Their relative instability is due to the presence of a greater amount of strained bonds (i.e. atoms in $3S$ or $2S + H$ environments) as compared to their neighbors. For example, $(AlOMe)_6$ contains $12(2S + H)$ atoms, $(AlOMe)_7$ contains $2(3S)$, $6(2S + H)$, and $6(2H + S)$ atoms and $(AlOMe)_8$ contains $8(2S + H)$ and $8(2H + S)$ atoms. Thus the presence of atoms in a $3S$ environment destabilizes $(AlOMe)_7$ in comparison with its neighbors. Note that eq 20 shows that for square and hexagonal faces only the order of stability is $3H > 2H + S > 2S + H > 3S$.

Consider the growth of a MAO cage by two monomer units as shown in Figure 9. All of these structures are composed of square and hexagonal faces. Clearly, such structural alternatives are possible for $(AlOMe)_{2n}$, where n = 3, 4, 5, ... Yet such structures contain six atoms in a $2S + H$ environment which is from an energetic perspective destabilizing. Other structural alternatives were found for $n > 10$. The entries given in Figure 8 for each n correspond to the most stable isomer.

Table 3. Comparison of Thermodynamic Properties Obtained Using UFF2 and ADF[a]

structure	ADF ZPE	UFF ZPE	ADF entropy	UFF entropy
$(AlOMe)_4$	100.14	98.87	126.221	130.880
$(AlOMe)_6$	148.21	149.12	162.206	159.012
$(AlOMe)_8$-II	197.89	198.81	211.609	207.582
$(AlOMe)_8$-III	198.72	199.46	219.594	221.281

[a] ZPE's given in kcal/mol; entropies in cal/molK at 298.15 K.

3.4. Enthalpic Considerations. Finite temperature enthalpies and entropies can be calculated from standard expressions[21] provided that all the vibrational frequencies are known (eqs 1−7 of the Supporting Information). Unfortunately, fully quantum mechanical frequency calculations are computationally expensive and would require too much time to be performed on all structures. Thus, another approach was taken, on the basis of molecular mechanics calculations using the universal force field.[18,19] First it was necessary to parametrize UFF2 so that the frequencies calculated agreed with those of ADF.

The original and optimized parameters of UFF2 are given in Tables 1.1−1.3 of the Supporting Information. The results of the ADF and UFF2 calculations for the parametrization are given in Table 3. It must be noted that the parametrization was performed on $(AlOMe)_4$ and $(AlOMe)_6$. It was then checked on $(AlOMe)_8$-II and $(AlOMe)_8$-III. As Table 3 shows, the parametrization reproduces zero-point energies and entropies of all of the structures extremely well. Moreover, it reproduces the differences for the two $(AlOMe)_8$ isomers. What must also be noted is the fact that the parametrization was performed on MAO structures which are composed solely of square and hexagonal faces. Yet, good values are also obtained for $(AlOMe)_8$-II which also contains two octagonal faces. Thus, these thermodynamic values obtained using UFF2 are quite reliable in the respect that they not only reflect the differences between isomers but also that they perform well for structures consisting of square, hexagonal, and octagonal faces.

The vibrational frequencies obtained via UFF2 were used to calculate the zero-point energies and finite temperature enthalpy corrections for the MAO structures. Next, formulas were found which could be used to predict these corrections. A full description of the fitting procedure can be found in the appendix. The total enthalpy is given as

$$H_T(n) = E(n) + H_{EC}(n) \tag{21a}$$

where $E(n)$ is the energy and $H_{EC}(n)$, the finite temperature enthalpy correction, is

$$H_{EC}(n) = H_{rot} + H_{trans} + H_{vib} \tag{21b}$$

Here H_{rot}, H_{trans}, and H_{vib} are the rotational, translational, and vibrational finite temperature enthalpy corrections, respectively.

(21) Hehre, W. J.; Radom, L.; Schleyer, P. V. R.; Pople, J. A. *Ab Initio Molecular Orbital Theory*; John Wiley & Sons: New York, 1986; pp 251, 259.

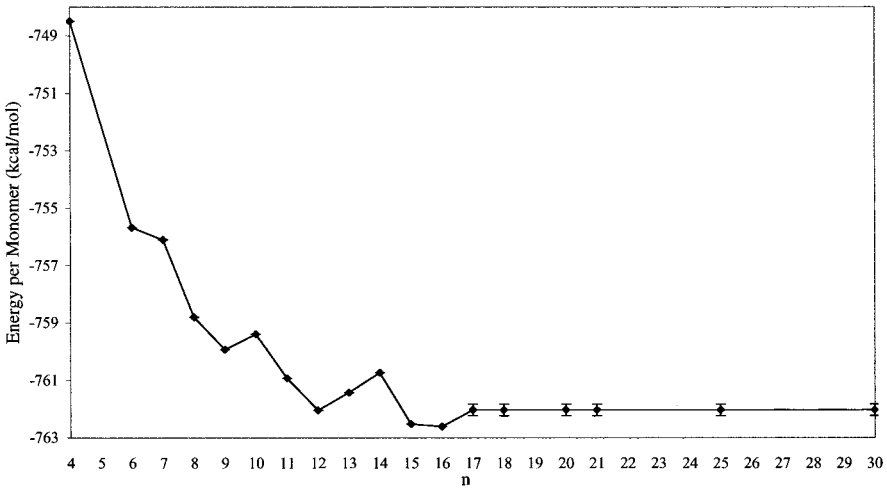

Figure 8. Energy per monomer vs *n*.

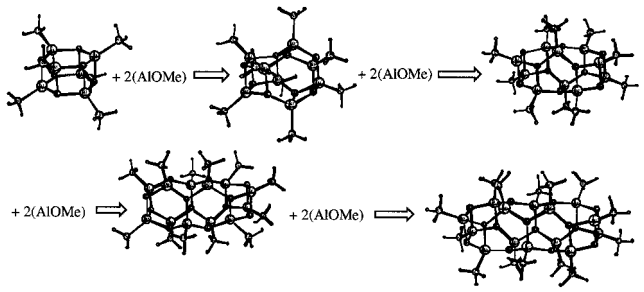

Figure 9. Growth of a MAO cage by 2 AlOMe units.

If H_0 is the zero-point energy, the parametrizations give the following in kcal/mol:

$$H_0 = 25n \tag{21c}$$

$$H_{rot} = H_{trans} = 3/2RT \tag{21d}$$

$$H_{vib} = H_0 + (0.0028T - 0.3548)n \ln(T) \tag{21e}$$

Note, T is in kelvin. Equation 21c gives an rms deviation of 1.16 kcal/mol, and eq 21d is exact, while the rms deviation for eq 21e is 3.28, 0.78, 1.32, and 3.36 kcal/mol at 198.15, 298.15, 398.15, and 598.15 K, respectively.

Figure 10 shows the finite temperature enthalpy correction per monomer unit ($H_{EC}(n)/n$) as a function of n at different temperatures. The values are plotted for oligomers composed of square and hexagonal faces only. Error bars are given for n = 17, 18, 20, 21, 25, and 30, where eqs 21c−e were used for predicting values. It shows that the enthalpy correction per monomer unit is almost the same for all MAO oligomers at the plotted temperatures. Hence, for a given disproportionation reaction $\Delta H_{EC}(n)$ will be nearly zero and does not contribute to the relative stability of the MAO oligomers.

3.5. Entropic Considerations. Entropic values were calculated via the parametrized UFF2 code. The total entropy of $(AlOMe)_n$ at temperature T is given by

$$S_T(n) = S_{trans} + S_{rot} + S_{vib} \tag{22a}$$

where S_{trans}, S_{rot}, and S_{vib} are the translational, rotational, and vibrational contributions to the entropy. The following equations predict the different entropic contributions at 298.15 K in cal/mol K (see Appendix for discussion of fit):

$$S_{trans} = 0.351n + 41.168 \tag{22b}$$

$$S_{rot} = 0.573n + 30.573 \tag{22c}$$

$$S_{vib} = 7.91(3S) + 8.30(2S + H) + 10.20(2H + S) + 8.49(3H) + 10.41(2S + O) + 9.50(2O + S) + 10.45(S + O + H) + 7.32(2H + O) + 0(2O + H) \tag{22d}$$

Here $3S$ corresponds to the number of atoms bonded to three square faces and so on. The rms deviation for S_{tot} is 1.78 kcal/mol at 298.15 K. Entropic corrections are temperature dependent, and hence, we devised equations which could be used to predict entropies at different temperatures given those at 298.15 K. They are the following in cal/mol K:

$$S_{2trans} = S_{1trans} + T_2/T_1 + (0.014)T_2 - 5.47 \tag{23a}$$

$$S_{2rot} = S_{1rot} + T_2/T_1 + (0.007)T_2 - 3.28 \tag{23b}$$

$$S_{2vib} = (T_2/T_1 - ((0.0006T_2^2 - 0.5353T_2 + 108.85)^{-1})S_{1vib} \tag{23c}$$

Here S_{2trans} is the translational entropy at temperature T_2 and so on. Equations 23a,b are nearly exact, while eq 23c gives an rms deviation of 0.27, 1.70, and 4.09 kcal/mol at 198.15, 398.15, and 598.15 K, respectively. Details of the fit can be found in the Appendix.

Figure 11 shows $-TS_T(n)/n$ as a function of n for different temperatures. For n = 17, 18, 20, 21, 25, and 30, eqs 22b−23c were used to predict the entropies; hence, only in these cases are error bars present. At low temperatures $-TS_T(n)/n$ is not very significant. As the temperature increases, $-TS_T(n)/n$ becomes more important in stabilizing smaller structures. At all temperatures the same trends are followed, yet the differences between adjacent points become greater with increasing temperature. The graph in Figure 11 displays an almost smooth curve, with a local minimum present at n = 12.

3.6. Gibbs Free Energy. The Gibbs free energy per monomer is given as

$$G_T(n)/n = H_T(n)/n - TS_T(n)/n \tag{24}$$

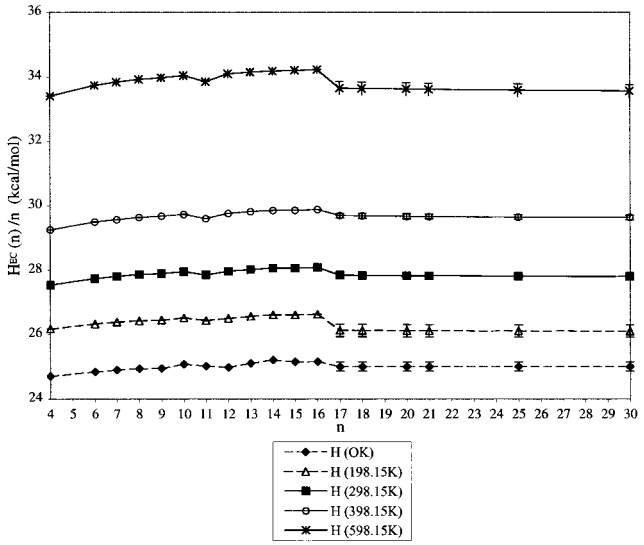

Figure 10. $H_{EC}(n)$ per monomer vs n.

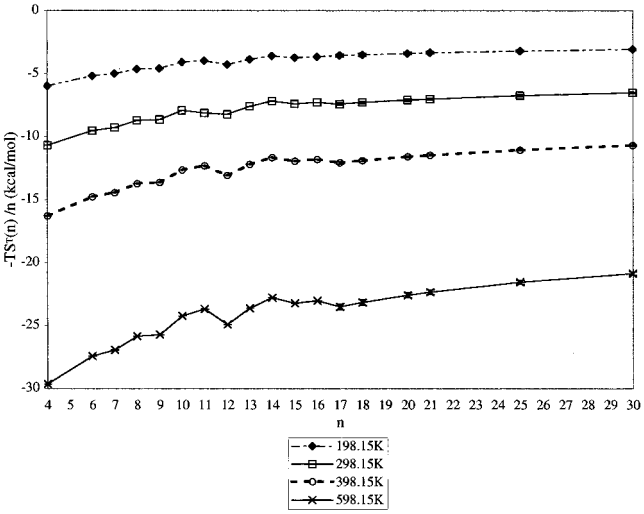

Figure 11. $-TS_T(n)$ per monomer vs n at different temperatures.

It is plotted in Figure 12 for structures composed of square and hexagonal faces only. It was found that these structures give the lowest Gibbs free energy for a given n, with one exception. That is of $(AlOMe)_{10}$ where another structure is 2.59 kcal/mol more stable. Error bars are present for $n = 17$, 18, 20, 21, 25, and 30, where eqs 15 and 16 were used to find the connectivities and the methods described earlier were used to estimate the Gibbs free energy. Table 3 of the Supporting Information gives the Gibbs free energy for all calculated structures at 298.15 K. Table 4 gives $G_T(n)/n$ for structures composed of square and hexagonal faces at all temperatures.

As can be noted, the same general trend is followed at all temperatures, with $(AlOMe)_{12}$ being the most stable. At lower temperatures, $(AlOMe)_{16}$ is almost as stable as $(AlOMe)_{12}$, while at high temperatures the difference increases. This can be attributed to entropic effects which were shown to be more important at higher temperatures. Local maxima at $n = 7$, 10, and 13 are present at all temperatures. They are due to energetic effects and appear as a consequence of the coefficients pertaining to each type of bonding environment present as can be seen in eq 5.

Equation 10 shows us that there are only six square faces present in a MAO structure composed of square and hexagonal faces only. Above we see that these structures have the lowest

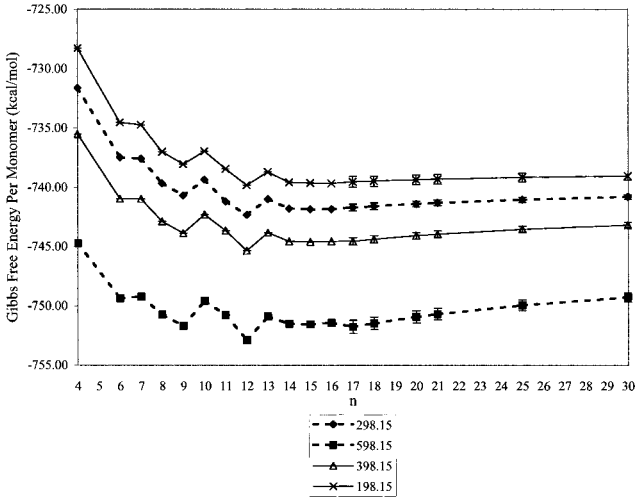

Figure 12. Gibbs free energy per monomer vs n at different temperatures.

Table 4. Percent Abundance of MAO at Different Temperatures

n	198.15 K	298.15 K	398.15 K	598.15 K
4	0.00	0.00	0.00	0.02
6	0.00	0.01	0.08	1.05
7	0.00	0.01	0.09	0.92
8	0.01	0.23	0.96	3.33
9	0.18	1.29	3.36	7.40
10	0.01	0.14	0.45	1.27
11	0.50	3.00	2.49	3.43
12	16.24	20.11	21.86	20.22
13	0.98	2.16	3.12	3.83
14	4.85	8.38	4.43	4.87
15	10.37	9.22	8.49	6.65
16	10.60	8.85	7.89	5.99
17	7.79	7.20	7.96	7.93
18	6.62	5.93	6.37	6.17
19	5.76	5.02	5.26	4.88
20	5.01	4.26	4.35	3.87
21	4.45	3.69	3.69	3.20
22	4.05	3.30	3.24	2.73
23	3.68	2.94	2.84	2.33
24	3.34	2.63	2.50	1.99
25	3.04	2.35	2.19	1.70
26	2.84	2.17	2.00	1.53
27	2.66	2.00	1.82	1.37
28	2.49	1.85	1.66	1.23
29	2.33	1.71	1.52	1.10
30	2.18	1.58	1.39	0.99

free energy for a given n. Moreover, the structures which are most stable do not have atoms in $3S$ or $2S + H$ environments; that is, they do not contain square-square edges. Due to the fact that these bonds are more strained and less stable they ought to be the sites with greatest latent Lewis acidity. Thus, we have shown that there are not many acidic or active sites in MAO. This topological consequence could be used to explain the high Al:catalyst ratio which is necessary for polymerization to occur.

The Gibbs free energy of $(AlOMe)_n$ relative to n monomeric units is given by

$$\Delta G_0(n) = G_T(n) - nG°T \qquad (25)$$

If $\Delta G_0(n)$ is defined in such a way, then eq 26 may be used to calculate equilibrium constants between $(AlOMe)_n$ and n monomer units. These are given in Table 5 of the Supporting Information. It must be noted that for $n = 17$, 18, 20, 21, 25, and 30 these were obtained via using the estimated Gibbs free energies for $(AlOMe)_n$. For $n = 19$, 22−24, and 26−29 the

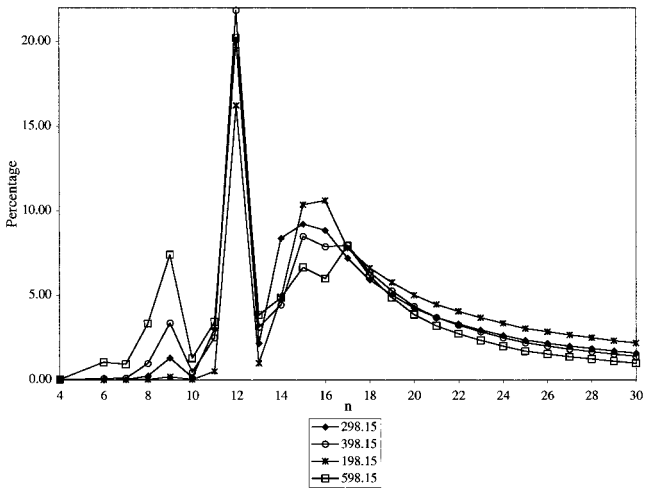

Figure 13. Percentage of each n at different temperatures.

Gibbs free energies were found via interpolation and next the equilibrium constants were calculated. As a check, structures were found via drawing a Schlegel diagram for $n = 19$, 22, and 24 and then the Gibbs free energy were predicted using the formulas given above. All of the Gibbs free energies found in such a manner fell within the error bars given when interpolation was done. Hence, this shows that it is valid to find the equilibrium constants for $n = 26-29$ in such a manner.

$$K_{eq} = \exp(-\Delta G_0(n)/RT) \tag{26}$$

Next, it is possible to find the percent abundance of a given structure according to eq 27. Table 4 gives the percent

$$\%(\mathrm{AlOMe})_n = (K_{eq}(n)/\sum_i K_{eq}(i)) \times 100 \tag{27}$$

abundance of the MAO's at different temperatures. This is also plotted in Figure 13. The most abundant species at all temperatures is $n = 12$, which ranges between 16 and 22%. Higher temperatures stabilize smaller species (which can be seen in the large increase of $n = 9$ at 598.15 K), while lower temperatures stabilize larger species (which can be seen in the increase of $n \geq 15$ at 198.15 K). This can also be seen when the weighted average of n is determined, which is 18.41, 17.23, 16.89, and 15.72 at 198.15, 298.15, 398.15, and 598.15 K, respectively. These values agree well with experimental data which estimate that n ranges between 14 and 20[10] especially considering the fact that only TMA-free MAO was examined in this study. However, it must be noted that it is not clear exactly what the experimental results show. That is, we are not sure if they report n for $(\mathrm{AlOMe})_n$, or $n + m$ for $(\mathrm{AlOMe})_n(\mathrm{TMA})_m$.

4. Conclusions

Within this study we have first of all proposed a method which can be used in theoretical structure determination. The method is based on drawing Schlegel diagrams and next constructing the appropriate three-dimensional object. We have also shown from topological arguments that in the most stable MAO structures there are only six square faces present and hence few square-square edges. These faces exhibit high ring strain, and hence, such edges/bonds would be the most acidic. We propose the low abundance of these faces and thus even a lower abundance of square-square edges to explain the high Al:catalyst ratio required for polymerization to occur. We have also provided a methodology which may be used to investigate any solution composed of an equilibrium mixture of oligomers.

Moreover, we have performed a complete study on pure MAO structures which consist of three-coordinate O and four-coordinate Al atoms. In so doing, we have fitted formulas which may be used to predict the energies, enthalpies, and entropies of any given MAO structure within the temperature range of 198.15−598.15 K effectively. Finally, we have calculated the percent distribution for each n within this temperature range. The weighted average gives n as 18.41, 17.23, 16.89, and 15.72 at 198.15, 298.15, 398.15, and 598.15 K, respectively. These values agree well with experimental data. However, it is not clear whether the experimental data gives values for n in $(\mathrm{AlOMe})_n$ or for $n + m$ in $(\mathrm{AlOMe})_n(\mathrm{TMA})_m$. Using some of the results obtained here, we shall in a forthcoming study discuss the structure of TMA-containing MAO.

Acknowledgment. This study was supported by the Natural Science and Engineering Research Council of Canada (NSERC) and by Novacor Research and Technology (NRTC) of Calgary, Alberta, Canada. Eva Zurek thanks NSERC for an undergraduate student scholarship. We thank Dr. Clark Landis of the University of Wisconsin for supplying us with UFF2 and Dr. Ted Bisztriczky of the University of Calgary Mathematics Department for his suggestion to use Schlegel diagrams for the construction of our MAO cages.

Appendix

We must first note that all temperatures are in K; all formulas predicting energies and enthalpies are in kcal/mol, and those predicting entropies in cal/mol K.

Energies. The energies of a given MAO caged structure were found to be heavily dependent upon the structure of the cage itself. For example, the energy difference between two $(\mathrm{AlOMe})_{12}$ isomers was found as being 59.8 kcal/mol. It was found that assigning certain coefficients to atoms in different bonding environments proved to be an effective means to predict energies. Of course, Al and O atoms are not equivalent and their positions within a certain bonding environment should add slightly different values to the energy. Only two cases were found where interchanging Al and O atoms gave different structures and, hence, where the geometries were not symmetric with respect to Al and O atoms. For $(\mathrm{AlOMe})_9$ they were structures **8** and **9** and for $(\mathrm{AlOMe})_{12}$ they are structures **17** and **18** of the Supporting Information. The energy differences between these two sets of structures were 3.2 and 7.6 kcal/mol, respectively. Such differences correspond to 0.05% and 0.08% of the total energy and hence are not very significant. Thus, it is reasonable to assume that Al and O atoms contribute by equal amounts to the energy of a given structure when found in a similar environment. In fact, the coefficients given in eq 20 correspond to an average value. Thus, the energies were fitted via a least-squares analysis, with the bonding environments as parameters. The bonding environments and fitted and calculated energies can be found in Table 6 of the Supporting Information.

Enthalpies. Table 7 of the Supporting Information shows that the zero-point enthalpy correction is $25n$, giving an rms deviation of 1.16 kcal/mol. Equations 5 and 6 of the Supporting Information show that modeling the translational and rotational contributions to the enthalpy is trivial. They are both given as $3/2RT$. The vibrational enthalpy was fitted for structures composed of square and hexagonal faces only. The fit was only performed on these structures since they have the lowest Gibbs free energy for a given n. The estimated and calculated values can be found in Table 8 of the Supporting Information.

Entropies. Equations 1 and 2 given in the Supporting Information show that the translational entropy is dependent only upon the mass of the molecule while the rotational entropy is dependent upon the moment of inertia, which is in turn dependent upon mass. Hence, it is natural to model the translational and rotational entropy as a function of n. Linear regression was used to obtain formulas which model these two parameters at room temperature to give eqs 22b and 22c.

The vibrational entropy varied considerably between different isomers and hence could not be modeled in a similar fashion. Thus, it was natural to model it in the same way as the energies. A least-squares analysis with the bonding environments as parameters was used to fit the entropies at 298.15 K. The results of the fits giving the translational, rotational, and vibrational entropies at room temperature are shown in Table 9 of the Supporting Information.

The extension to different temperatures was performed on structures consisting only of square and hexagonal faces. Since predicting entropies at 298.15 K was already possible, it was decided to devise a method by which entropies at different temperatures could be found using these values. Tables 10 and 11 of the Supporting Information give the predicted and calculated values for translational and rotational entropies.

To predict vibrational entropies at a variety of different temperatures, a different approach must be taken. From eq 3 of the Supporting Information, we are given the vibrational entropy at one temperature. If we assume that the entropy at another temperature is proportional to this value, the following equation is obtained:

$$nR\Sigma\{(u_{(i)1}e^{u(i)1} - 1)^{-1} - \ln(1 - e^{-u(i)1})\} = C[nR\Sigma\{(u_{(i)2}e^{u(i)2} - 1)^{-1} - \ln(1 - e^{-u(i)2})\}] \quad (28)$$

Here C is some constant to be determined and $u_{(i)} = h\nu_{(i)}/kT$.

Hence, for a given ν,

$$\{(h\nu_1/kT_1 \exp(h\nu_1/kT_1) - 1)^{-1} - \ln(1 - \exp(-h\nu_1/kT_1)\} = C\{(h\nu_1/kT_2 \exp(h\nu_1/kT_2) - 1)^{-1} - \ln(1 - \exp(-h\nu_1/kT_2)\} \quad (29)$$

Since $h\nu/kT$ is of the order of magnitude of about 10, we can assume that $\exp(-h\nu_1/kT_1) \rightarrow 0$. Thus, $\ln(1 - \exp(-h\nu/kT) = \ln(1) = 0$. If one simplifies eq 29 and solves for C, the following is obtained:

$$C = \{h\nu_1/kT_2 \exp(h\nu_1/kT_2)\}/\{h\nu_1/kT_1 \exp(h\nu_1/kT_1)\} \quad (30)$$

$$C = (T_1/T_2) \exp(h\nu_1/k\,(1/T_2 - 1/T_1)) \quad (31)$$

Using a Taylor series expansion,

$$C = (T_1/T_2)(1 + \text{higher order terms}) \quad (32)$$

The higher order terms contain ν_1 and hence will be neglected. Instead, a small correction factor will be added to eq 32 in order to compensate for neglecting these terms. The correction factor was found as being $(0.0006T^2 - 0.5353T + 108.85)^{-1}$. Thus, the vibrational entropies may be obtained via the following equation:

$$S_2 = T_2/T_1 - ((0.0006T_2^{\,2} - 0.5353T_2 + 108.85)^{-1})S_1 \quad (33)$$

Table 12 of the Supporting Information shows the differences between calculated vibrational entropies and those estimated using eq 33. The rms deviations were found as being 0.27, 1.70, and 4.09 kcal/mol for 198.15, 398.15, and 598.15 K, respectively. This also gives a good fit, especially taking into account the fact that the entropies were estimated accurately over a 400 K temperature range. It must be noted that as the temperature rises, the approximation that $\exp(-h\nu_1/kT_1) \rightarrow 0$ becomes less appropriate. This is why the rms deviation increases with increasing temperature and becomes comparably quite large at 598.15 K.

Supporting Information Available: Equations used to calculate thermodynamic properties, diagrams of all computed MAO caged structures, Cartesian coordinates of all optimized structures, optimized parameters for UFF2, binding energies per monomer for all MAO caged structures, Gibbs free energies for all MAO structures at 298.15 K; Gibbs free energy per monomer unit for MAO caged structures composed of square and hexagonal faces only within the temperature range of 198.15−598.15 K, equilibrium constants for the reaction $n(\text{AlOMe}) \rightarrow (\text{AlOMe})_n$ within the temperature range of 198.15−598.15 K, bonding environments and fitted energies for all structures, calculated and predicted zero-point energies for all structures, predicted and calculated vibrational enthalpies at different temperatures, predicted and calculated entropy values at 298.15 K, and predicted and calculated translational, rotational, and vibrational entropies at different temperatures. This material is available free of charge via the Internet at http://pubs.acs.org.

IC000845B